A comparison between scalp- and source-reconstructed EEG networks

Margherita Lai[1], Matteo Demuru[2], Arjan Hillebrand[2], Matteo Fraschini[1,*]

[1] Department of Electrical and Electronic Engineering, University of Cagliari, Piazza D'armi, Cagliari, I-09123, Italy

[2] Department of Clinical Neurophysiology and MEG Center, VU University Medical Centre, Amsterdam, The Netherlands

[*] **Corresponding author:**

Matteo Fraschini
Department of Electrical and Electronic Engineering
University of Cagliari
Piazza D'armi
Cagliari, I-09123
Italy
Tel. +39 070 675 5894
email. fraschin@unica.it

Abstract

Modern network science is a fundamental tool for the understanding of brain organization. EEG recordings of brain activity can be used to reconstruct, and characterise, functional networks using a variety of connectivity metrics and measures of network topology. Unlike EEG source reconstruction techniques, scalp analysis does not allow to make inferences about interacting anatomical regions, yet this latter approach has not been abandoned. Although the two approaches use different assumptions, conclusions drawn regarding the (global) topology of the underlying networks should, ideally, not depend on the approach that is used. Our aim was to compare network measures, as defined by minimum spanning tree (MST) parameters, extracted from scalp and source EEG signals, using a variety of functional connectivity (FC) metrics. Eyes-closed resting-state EEG recordings from 109 subjects were analysed with amplitude- and phase-based FC metrics, both with and without correction for field spread and volume conduction/signal leakage. We found a strong correlation (0.849<rho<0.933) for the global mean connectivity between scalp- and source-level for all the FC metrics. In contrast, network topology was only weakly correlated. The strongest correlations (0.262<rho<0.346) were obtained for MST leaf fraction, but only for connectivity metrics that limit the effects of field spread and volume conduction/signal leakage. These findings suggest that the effects of field spread and volume conduction/leakage alter the estimated scalp EEG network organization, thereby limiting the interpretation of results of EEG scalp analysis. Finally, this study also suggests that the use of metrics that address the problem of zero lag correlations may give more reliable estimates of the topology of the underlying brain networks.

Keywords: EEG, scalp, source, functional connectivity, network topology, Minimum Spanning Tree.

Introduction

Modern network science is a fundamental tool for the understanding of both normal and abnormal brain organization (Bullmore and Sporns, 2009; Sporns et al., 2004; Stam, 2014). In this context, alongside other imaging techniques such as magnetoencephalography (MEG) and functional MRI (fMRI), electroencephalography (EEG) has been widely used to study brain networks (Stam, 2014; Stam and van Straaten, 2012). It is well accepted that scalp-level EEG analysis does not allow inferences in terms of underlying neuroanatomy (Steen et al., 2016), thus suggesting the use of source reconstruction techniques (Schoffelen and Gross, 2009), yet the former approach has not been abandoned. The main problems with scalp-level analysis of functional networks are related to two considerations: i) the already mentioned problem that location of EEG channels do not relate trivially to the location of the underlying sources; and ii) spurious estimates of functional connectivity can occur between the channels due to the effects of field spread (Dominguez et al., 2007) and volume conduction (Schoffelen and Gross, 2009), where more than one channel can pick up the activity of an underlying source, although these effects can still be present in source-space (Brookes et al., 2014), where it is often referred to as signal leakage. Although scalp- and source-level analyses use different assumptions, conclusions drawn regarding the (global) topology of the underlying networks should, ideally, not depend on the approach that is used.

The aim of the present paper was to compare network measures extracted from scalp and source EEG signals, as defined by the minimum spanning tree (MST), and using a variety of functional connectivity (FC) metrics. The MST represents a network approach that provides an unbiased reconstruction of the core of a network (Stam et al., 2014; Tewarie et al., 2015). MST parameters are sensitive to alterations in network topology (Tewarie et al., 2015) and several studies have already implemented this approach in order to study network alteration at the scalp- (Crobe et al., 2016; Demuru et al., 2013; Fraga González et al., 2016; Fraschini et al., 2016b, 2015, 2014; van Diessen et al., 2016; Vourkas et al., 2014; Yu et al., 2016) and source-level (Dubbelink et al., 2014; Nissen et al., 2017; Tewarie et al., 2014; van Dellen et al., 2014). Under certain conditions, the

MST forms the critical backbone of the original network (Van Mieghem and Magdalena, 2005; Van Mieghem and van Langen, 2005; Wang et al., 2008). Moreover, it addresses several methodological limitations (i.e. biased estimates of network topology due to differences in connection strength or link density) (van Wijk et al., 2010), yet still captures changes in topology of the original network (Tewarie et al., 2015).

In order to assess the effect of field spread and volume conduction/leakage we included FC metrics that are sensitive to these effects, namely the phase locking value (PLV) (Lachaux et al., 1999) and the amplitude envelope correlation (AEC) (Brookes et al., 2011), and metrics that are relatively insensitive to these effects, namely the phase lag index (PLI) (Stam et al., 2007) and AEC after leakage correction (Brookes et al., 2011; Hipp et al., 2012). Subsequently, several MST parameters were used to characterize the global topology of the reconstructed functional networks.

We used a freely available EEG dataset (Goldberger et al., 2000; Schalk et al., 2004) that includes one minute eyes-closed resting-state recordings from 109 subjects. Source-level time-series of neuronal activity were reconstructed for 68 ROIs (Desikan et al., 2006) by means of the weighted Minimum Norm Estimate (wMNE) (Fuchs et al., 1999; Hämäläinen, 1984; Hämäläinen and Ilmoniemi, 1994; Lin et al., 2006) and segmented into five non-overlapping epochs. MSTs were reconstructed for four FC metrics, both at the scalp- and source-level, and parameters that characterise global topology were subsequently compared between the two domains.

Material and methods

Dataset

A dataset created by the developers of the BCI2000 instrumentation system, consisting of 64-channels EEG recordings from 109 subjects, was used in this study (Goldberger et al., 2000; Schalk et al., 2004). The dataset contains fourteen different experimental runs for each subject, comprising of two one-minute baseline runs (eyes-open and eyes-closed resting-state conditions). For the aim of the present work, we considered only the eyes-closed resting-state runs. The data are provided in EDF+ format and contain 64 raw EEG signals as per the international 10-10 system, sampled at 160 Hz.

EEG pre-processing

EEGLAB (version 13_6_5b) (Delorme and Makeig, 2004) was used to re-reference and filter (with *fir1* filter type) the EEG signals (band-pass filter between 1 and 70 Hz and 60 Hz notch filtering). Successively, ADJUST (version 1.1.1) (Mognon et al., 2011), a fully automatic algorithm based on Independent Component Analysis (ICA), was used to detect and remove artefacts from the filtered signals.

Source reconstruction

Source-reconstructed time-series were obtained by using Brainstorm software (version 3.4) (Tadel et al., 2011). First, a head model was created using a symmetric boundary element method in Open-MEEG (version 2.3.0.1) (Gramfort et al., 2010; Kybic et al., 2005) based on the anatomy derived from the ICBM152 brain (Mazziotta et al., 2001). Time-series of neuronal activity were reconstructed using whitened and depth-weighted linear L2 minimum norm estimate (wMNE) (Fuchs et al., 1999; Hämäläinen, 1984; Hämäläinen and Ilmoniemi, 1994; Lin et al., 2006), with an

identity matrix as noise covariance. Sources were constrained to the cortex and source orientation was perpendicular to the cortical surface (Mosher et al., 1999). To limit the effect of differences in network size (van Wijk et al., 2010) between scalp- (64 channels) and source-analysis, source-reconstructed time-series were projected onto 68 regions of interest (ROIs) as defined by the Desikan-Killiany atlas (Desikan et al., 2006), where time-series for voxels within a ROI were averaged (after flipping the sign of sources with opposite directions).

Connectivity metrics

Functional connectivity metrics that are either sensitive or insensitive to the effects of field spread and volume conduction/signal leakage, based on either amplitude or phase information, were used. In particular, we used AEC, a measure of amplitude coupling that uses linear correlations of the envelopes of the band-pass filtered signals (Brookes et al., 2011; Hipp et al., 2012) and $AEC_{corrected}$, a version that uses a symmetric orthogonalisation procedure to remove zero-lag correlations (implemented in the time domain (Hipp et al., 2012)). Furthermore, we used the PLV (Lachaux et al., 1999), a measure that quantifies the consistency of phase differences (including zero-lag), and the PLI (Stam et al., 2007), a measure that quantifies the asymmetry of the distribution of phase differences between time series and that ignores zero-lag phase differences. The connectivity metrics were calculated for all epochs of each subject, after having band-pass filtered the scalp- or source-reconstructed time-series in the alpha band (8-13 Hz) and segmenting the one-minute recordings in five non-overlapping epochs of 12 seconds (Fraschini et al., 2016a).

Functional Network Topology

The EEG channels (scalp-level analysis) and the atlas-based ROIs (source-level analysis) were considered as network nodes, and the functional connections as weighted edges within the network. Then the MST, a sub-network that connects all nodes whilst minimizing the link weights without forming loops, was reconstructed. Since we are interested in the strongest connections, the

connection weights were inverted (1 – FC measure) before constructing the MST. The topology of the MST was characterised using the following parameters (Boersma et al., 2013): the leaf fraction (number of nodes with degree of 1 divided by the total number of nodes), the diameter (largest distance between any two nodes), the tree hierarchy (balance between hub overload and network integration) and the kappa (broadness of degree distribution). All analyses were performed using Matlab R2016b (The MathWorks, Inc., Natick, Massachusetts, US) and the MIT Strategic Engineering Matlab Tools for Network Analysis (Bounova and de Weck, 2012).

Statistical analysis

Correlations between scalp- and source-derived measures were assessed using Spearman's rank correlation coefficient. In order to test differences between correlations from the different connectivity approaches, the ones that are insensitive to zero-lag correlations in contrast to the ones that are sensitive, we used a percentile bootstrap approach for non-overlapping correlations (Wilcox, 2016), using 500 repetitions, and using the code available at https://github.com/GRousselet/blog/tree/master/comp2dcorr and described at https://garstats.wordpress.com/2017/03/01/comp2dcorr/.

Results

The associations between measures extracted from scalp- and source-reconstructed networks are represented as scatterplot in Figure 1. The Spearman correlations between scalp- and source-level global average connectivity was high for all connectivity metrics, whereas correlations were low to moderate for the MST parameters. For the MSTs, the highest correlations were observed for leaf fraction for MSTs based on $AEC_{corrected}$ (rho = 0.346) and PLI (rho = 0.262).

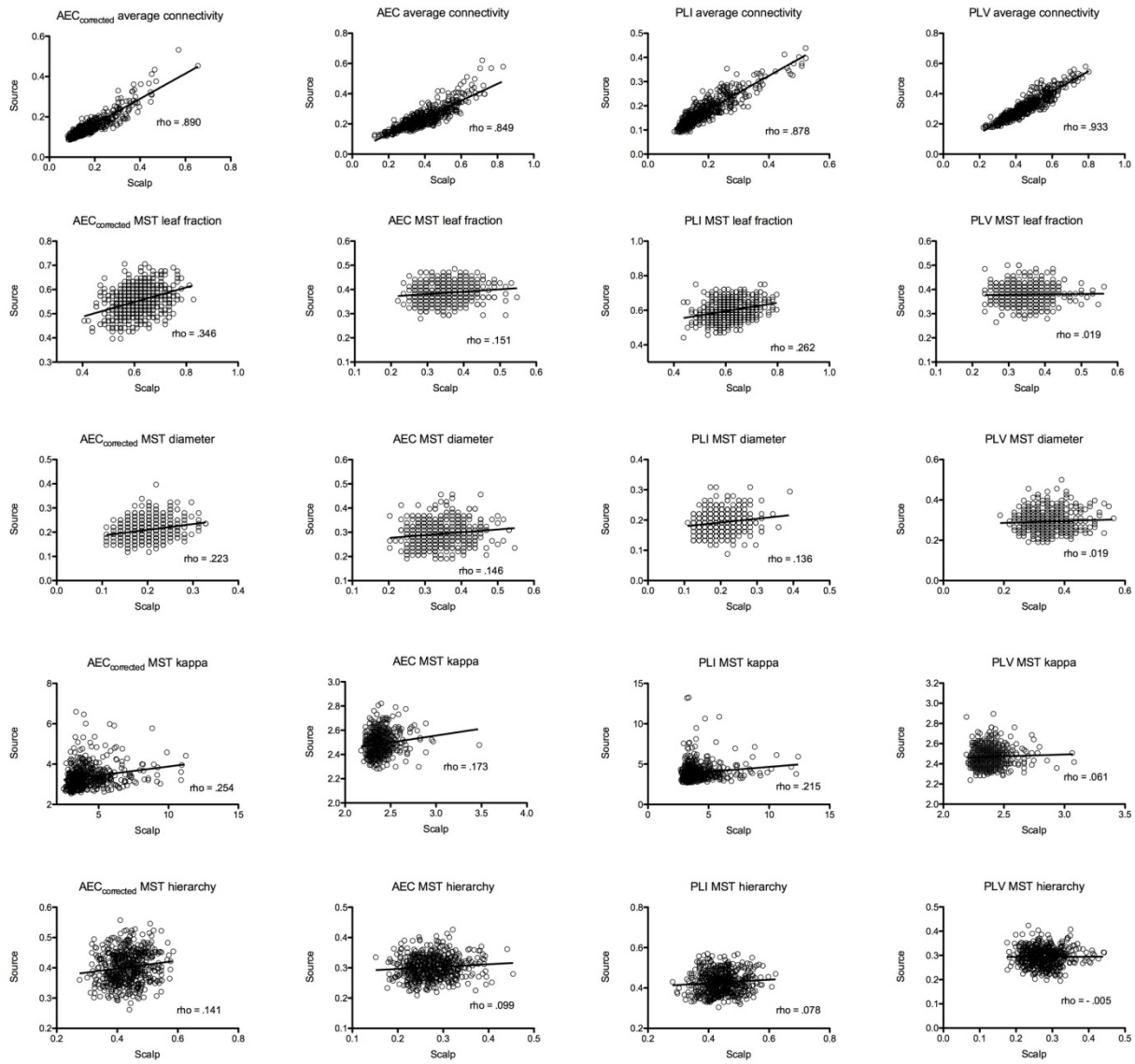

Figure 1. Scatterplots of scalp- and source-based measures of FC and network topology. The strength of the correlation is reported as rho value. Note that estimates of network topology only correlated weakly to moderately (maximum rho = 0.346) between scalp- and source-level, even though average FC correlated strongly.

For all the MST parameters, MSTs based on $AEC_{corrected}$ and PLI showed higher correlations in comparison with AEC and PLV. In particular, PLV-based MST parameters showed the lowest correlations, with correlations strength approaching zero for all the evaluated network measures (maximum rho = 0.061, for MST kappa). Statistical differences, expressed using confidence intervals, between Spearman correlations derived from amplitude and phase based coupling approaches are summarized in Table1 and Table 2. For amplitude based FC metrics, the largest difference was observed for MST leaf fraction, whilst for the other MST parameters the differences were small. For phase-based FC metrics, the most marked differences were observed for MST leaf fraction and MST Kappa. For both the amplitude- and phase-based approaches, the MST Hierarchy showed only minimal differences. Figure 2 shows differences and bootstrap distributions for MST leaf fraction, for MSTs based on $AEC_{corrected}$ versus AEC (left panel) and for MSTs based on PLI versus PLV (right panel).

	$AEC_{corrected}$	**AEC**	**Statistics**	
	rho	*rho*	*difference*	*CI*
MST leaf fraction	0.346	0.151	0.195	[0.08 0.32]
MST diameter	0.223	0.146	0.078	[-0.03 0.18]
MST kappa	0.254	0.173	0.081	[-0.03 0.19]
MST hierarchy	0.141	0.099	0.043	[-0.07 0.15]

Table 1. Comparison between scalp- and source-level correlations for amplitude based FC metrics. Mean difference and confidence intervals are reported.

	PLI	**PLV**	**Statistics**	
	rho	*rho*	*difference*	*CI*
MST leaf fraction	0.262	0.019	0.243	[0.13 0.37]
MST diameter	0.136	0.019	0.117	[0.00 0.23]
MST kappa	0.215	0.061	0.153	[0.03 0.27]
MST hierarchy	0.078	-0.005	0.082	[-0.04 0.19]

Table 2. Comparison between scalp- and source-level correlations for phase based FC metrics. Mean difference and confidence intervals are reported.

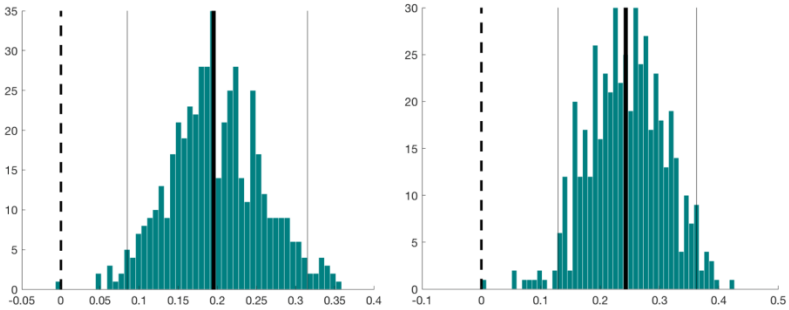

Figure 2. Differences and bootstrap distributions for MST leaf fraction, for $AEC_{corrected}$ versus AEC (left panel) and for PLI versus PLV (right panel). The difference between coefficients is marked by a thick vertical black line. The 95% percentile bootstrap confidence interval is illustrated by the two thin vertical black lines.

Discussion

Although network reconstructions at the scalp- and source-level rely on different assumptions, conclusions drawn regarding the (global) topology of the underlying networks should, ideally, not depend on the approach that is used. We found that average functional connectivity correlated strongly between the two domains, independent of the metric that was used. In contrast, global MST network descriptors extracted from scalp- and source-level EEG signals correlated (at best) moderately. In particular, in the case of connectivity metrics that do not limit spurious connections that are due to field spread and volume conduction/signal leakage (PLV and uncorrected version of AEC), the correlations were particularly weak. Although topological parameters for MSTs based on $AEC_{corrected}$ and PLI showed only moderate correlations between scalp- and source-level, they were still higher than for MSTs based on PLV and uncorrected AEC for all of the estimated network measures. These differences (between scalp-/sensor-level correlations) were most evident for phase-based synchronization metrics, where PLI allowed to obtain higher correlations than PLV, for two of the MST descriptors (leaf fraction and kappa). These findings, which show minimal consistency between network analysis at scalp- and source-level, still advise against the use of FC metrics that do not correct for spurious correlations as they tend to amplify the differences between the two domains (scalp- and source-level). Conversely, the use of metrics that limit spurious connectivity ($AEC_{corrected}$ and PLI) tends to reduce these differences.

In this work, we used weighted minimum norm estimated to reconstruct the source activity. It should be noted that different source reconstruction methods (Baillet et al., 2001), such as beamforming (Hillebrand et al., 2005), may provide different results in terms of global network topology and the correlation between scalp- and sensor-level estimates, since beamformer reconstructions may provide a more robust demixing of the time-series (i.e., separating the contribution from different underlying sources to a single sensor) compared to the relatively smooth solutions that are obtained with wMNE (Hillebrand and Barnes, 2005). Since the accuracy of source localization may increase with the number of channels (Antiqueira et al., 2010; Lantz et al., 2003),

one would expect the correlations between networks reconstructed at the sensor- and source-level to be higher for MEG than for EEG. The reduced sensitivity of MEG volume conduction may further aid in this respect.

The present work suffers from some limitations. First of all, there was no ground truth in our study, and the interpretation of our results is based on the assumption that network estimates at the source-level are a better approximation of the unknown true network organization than scalp-level estimates. This assumption is in line with a previous study (Antiqueira et al., 2010) that have highlighted that scalp-level network analyses may result in erroneous inferences about the underlying network topology. In particular, the model study by Antiqueira and colleagues suggests that scalp-based network structures, especially when under-sampled at surface sites, might not agree with the underlying three-dimensional network. Another limitation refers to the inherently different mapping approaches between scalp- (channels) and source-level (ROIs) analysis, that strongly hinder the comparison between the two domains. Even though the number of EEG channels differed only slightly from the number of reconstructed ROIs (64 versus 68), it has been shown that differences in network size can affect estimates of network topology (van Wijk et al., 2010). The correlations between the scalp- and source-level estimates of network topology presented here may therefore be lower than those that would have been obtained in case the networks had been of equal size. Another consideration is that consistency for local measures (e.g. nodal centrality) may be lower than reported for the global network measures. Finally, the ICA-based artefact-rejection that we used may have distorted the phases (Castellanos and Makarov, 2006). However, since our study is focused on the comparison between analyses at the scalp- and source-level, and is not intended to unveil the true underlying network topology, this limitation should only slightly impact on the reported results. Future studies should elucidate the effects of ICA artefact-rejection on subsequent connectivity and network analyses.

In conclusion, the present work confirms that, although functional connectivity can be estimated reliably, extreme caution should be used when interpreting results derived from scalp-

level EEG network analysis, even when unbiased approaches such as MST analysis are used. However, assuming that the source-based network representation is a better approximation of the unknown true network organization, our findings also indicate that connectivity metrics that limit the emergence of spurious correlations (such as the corrected AEC and PLI) may allow for more reliable estimates of the underlying global network organization.

Reference

Antiqueira, L., Rodrigues, F.A., van Wijk, B.C.M., Costa, L. da F., Daffertshofer, A., 2010. Estimating complex cortical networks via surface recordings—A critical note. Neuroimage 53, 439–449. doi:10.1016/j.neuroimage.2010.06.018

Baillet, S., Mosher, J.C., Leahy, R.M., 2001. Electromagnetic brain mapping. IEEE Signal Process. Mag. 18, 14–30. doi:10.1109/79.962275

Boersma, M., Smit, D.J.A., Boomsma, D.I., De Geus, E.J.C., Delemarre-van de Waal, H.A., Stam, C.J., 2013. Growing trees in child brains: graph theoretical analysis of electroencephalography-derived minimum spanning tree in 5- and 7-year-old children reflects brain maturation. Brain Connect. 3, 50–60. doi:10.1089/brain.2012.0106

Bounova, G., de Weck, O., 2012. Overview of metrics and their correlation patterns for multiple-metric topology analysis on heterogeneous graph ensembles. Phys. Rev. E 85, 16117. doi:10.1103/PhysRevE.85.016117

Brookes, M., Woolrich, M., Price, D., 2014. An Introduction to MEG connectivity measurements, in: Magnetoencephalography. Springer Berlin Heidelberg, pp. 321–358.

Brookes, M.J., Hale, J.R., Zumer, J.M., Stevenson, C.M., Francis, S.T., Barnes, G.R., Owen, J.P., Morris, P.G., Nagarajan, S.S., 2011. Measuring functional connectivity using MEG: Methodology and comparison with fcMRI. Neuroimage 56, 1082–1104. doi:10.1016/j.neuroimage.2011.02.054

Bullmore, E., Sporns, O., 2009. Complex brain networks: graph theoretical analysis of structural and functional systems. Nat. Rev. Neurosci. 10, 186–98. doi:10.1038/nrn2575

Castellanos, N.P., Makarov, V.A., 2006. Recovering EEG brain signals: Artifact suppression with wavelet enhanced independent component analysis. J. Neurosci. Methods 158, 300–312. doi:10.1016/j.jneumeth.2006.05.033

Crobe, A., Demuru, M., Didaci, L., Marcialis, G.L., Fraschini, M., 2016. Minimum spanning tree and k -core decomposition as measure of subject-specific EEG traits. Biomed. Phys. Eng. Express 2, 17001. doi:10.1088/2057-1976/2/1/017001

Delorme, A., Makeig, S., 2004. EEGLAB: an open source toolbox for analysis of single-trial EEG dynamics including independent component analysis. J. Neurosci. Methods 134, 9–21. doi:10.1016/j.jneumeth.2003.10.009

Demuru, M., Fara, F., Fraschini, M., 2013. Brain network analysis of EEG functional connectivity during imagery hand movements. J. Integr. Neurosci. 12, 441–7. doi:10.1142/S021963521350026X

Desikan, R.S., Ségonne, F., Fischl, B., Quinn, B.T., Dickerson, B.C., Blacker, D., Buckner, R.L., Dale, A.M., Maguire, R.P., Hyman, B.T., Albert, M.S., Killiany, R.J., 2006. An automated labeling system for subdividing the human cerebral cortex on MRI scans into gyral based regions of interest. Neuroimage 31, 968–980. doi:10.1016/j.neuroimage.2006.01.021

Dominguez, L.G., Wennberg, R., Velazquez, J.L.P., Erra, R.G., 2007. Enhanced measured synchronization of unsynchronized sources: inspecting the physiological significance of synchronization analysis of whole brain electrophysiological recordings. Int. J. Phys. Sci. 2, 305–317. doi:10.1186/1471-2202-8-S2-P41

Dubbelink, K.T.E.O., Hillebrand, A., Stoffers, D., Deijen, J.B., Twisk, J.W.R., Stam, C.J., Berendse, H.W., 2014. Disrupted brain network topology in Parkinson ' s disease : a longitudinal magnetoencephalography study. Brain 197–207. doi:10.1093/brain/awt316

Fraga González, G., Van der Molen, M.J.W., Žarić, G., Bonte, M., Tijms, J., Blomert, L., Stam, C.J., Van der Molen, M.W., 2016. Graph analysis of EEG resting state functional networks in dyslexic readers. Clin. Neurophysiol. 127, 3165–3175. doi:10.1016/j.clinph.2016.06.023

Fraschini, M., Demuru, M., Crobe, A., Marrosu, F., Stam, C.J., Hillebrand, A., 2016a. The effect of epoch length on estimated EEG functional connectivity and brain network organisation. J. Neural Eng. 13, 36015. doi:10.1088/1741-2560/13/3/036015

Fraschini, M., Demuru, M., Hillebrand, A., Cuccu, L., Porcu, S., Di Stefano, F., Puligheddu, M., Floris, G., Borghero, G., Marrosu, F., 2016b. EEG functional network topology is associated with disability in patients with amyotrophic lateral sclerosis. Sci. Rep. 6, 38653. doi:10.1038/srep38653

Fraschini, M., Demuru, M., Puligheddu, M., Floridia, S., Polizzi, L., Maleci, A., Bortolato, M., Hillebrand, A., Marrosu, F., 2014. The re-organization of functional brain networks in pharmaco-resistant epileptic patients who respond to VNS. Neurosci. Lett. 580, 153–7. doi:10.1016/j.neulet.2014.08.010

Fraschini, M., Hillebrand, A., Demuru, M., Didaci, L., Marcialis, G.L., 2015. An EEG-Based Biometric System Using Eigenvector Centrality in Resting State Brain Networks. IEEE Signal Process. Lett. 22, 666–670. doi:10.1109/LSP.2014.2367091

Fuchs, M., Wagner, M., Köhler, T., Wischmann, H.A., 1999. Linear and nonlinear current density reconstructions. J. Clin. Neurophysiol. 16, 267–95.

Goldberger, A.L., Amaral, L.A.N., Glass, L., Hausdorff, J.M., Ivanov, P.C., Mark, R.G., Mietus, J.E., Moody, G.B., Peng, C.-K., Stanley, H.E., 2000. PhysioBank, PhysioToolkit, and PhysioNet : Components of a New Research Resource for Complex Physiologic Signals. Circulation 101, e215–e220. doi:10.1161/01.CIR.101.23.e215

Gramfort, A., Papadopoulo, T., Olivi, E., Clerc, M., 2010. OpenMEEG: opensource software for quasistatic bioelectromagnetics. Biomed. Eng. Online 9, 45. doi:10.1186/1475-925X-9-45

Hämäläinen, M.S., 1984. Interpreting measured magnetic fields in the brain: Estimates of current distributions. Technical Report TKK-F-A559, Helsinki University of Technology.

Hämäläinen, M.S., Ilmoniemi, R.J., 1994. Interpreting magnetic fields of the brain: minimum norm estimates. Med. Biol. Eng. Comput. 32, 35–42. doi:10.1007/BF02512476

Hillebrand, A., Barnes, G., 2005. Beamformer Analysis of MEG Data. Int. Rev. Neurobiol. 68, 149–171. doi:10.1016/S0074-7742(05)68006-3

Hillebrand, A., Singh, K.D., Holliday, I.E., Furlong, P.L., Barnes, G.R., 2005. A new approach to neuroimaging with magnetoencephalography. Hum. Brain Mapp. 25, 199–211. doi:10.1002/hbm.20102

Hipp, J.F., Hawellek, D.J., Corbetta, M., Siegel, M., Engel, A.K., 2012. Large-scale cortical correlation structure of spontaneous oscillatory activity. Nat. Neurosci. 15, 884–890. doi:10.1038/nn.3101

Kybic, J., Clerc, M., Abboud, T., Faugeras, O., Keriven, R., Papadopoulo, T., 2005. A common formalism for the Integral formulations of the forward EEG problem. IEEE Trans. Med. Imaging 24, 12–28. doi:10.1109/TMI.2004.837363

Lachaux, J.P., Rodriguez, E., Martinerie, J., Varela, F.J., 1999. Measuring phase synchrony in brain signals. Hum. Brain Mapp. 8, 194–208.

Lantz, G., Grave de Peralta, R., Spinelli, L., Seeck, M., Michel, C.., 2003. Epileptic source localization with high density EEG: how many electrodes are needed? Clin. Neurophysiol. 114, 63–69. doi:10.1016/S1388-2457(02)00337-1

Lin, F.-H., Witzel, T., Ahlfors, S.P., Stufflebeam, S.M., Belliveau, J.W., Hämäläinen, M.S., 2006. Assessing and improving the spatial accuracy in MEG source localization by depth-weighted minimum-norm estimates. Neuroimage 31, 160–171. doi:10.1016/j.neuroimage.2005.11.054

Mazziotta, J., Toga, A., Evans, A., Fox, P., Lancaster, J., Zilles, K., Woods, R., Paus, T., Simpson, G., Pike, B., Holmes, C., Collins, L., Thompson, P., MacDonald, D., Iacoboni, M., Schormann, T., Amunts, K., Palomero-Gallagher, N., Geyer, S., Parsons, L., Narr, K., Kabani, N., Le Goualher, G., Feidler, J., Smith, K., Boomsma, D., Hulshoff Pol, H., Cannon, T., Kawashima, R., Mazoyer, B., 2001. A four-dimensional probabilistic atlas of the human brain. J. Am. Med. Inform. Assoc. 8, 401–30.

Mognon, A., Jovicich, J., Bruzzone, L., Buiatti, M., 2011. ADJUST: An automatic EEG artifact detector based on the joint use of spatial and temporal features. Psychophysiology 48, 229–240. doi:10.1111/j.1469-8986.2010.01061.x

Mosher, J.C., Leahy, R.M., Lewis, P.S., 1999. EEG and MEG: forward solutions for inverse methods. IEEE Trans. Biomed. Eng. 46, 245–59.
Nissen, I.A., Stam, C.J., Reijneveld, J.C., van Straaten, I.E.C.W., Hendriks, E.J., Baayen, J.C., De Witt Hamer, P.C., Idema, S., Hillebrand, A., 2017. Identifying the epileptogenic zone in interictal resting-state MEG source-space networks. Epilepsia 58, 137–148. doi:10.1111/epi.13622
Schalk, G., McFarland, D.J., Hinterberger, T., Birbaumer, N., Wolpaw, J.R., 2004. BCI2000: a general-purpose brain-computer interface (BCI) system. IEEE Trans. Biomed. Eng. 51, 1034–43. doi:10.1109/TBME.2004.827072
Schoffelen, J.-M., Gross, J., 2009. Source connectivity analysis with MEG and EEG. Hum. Brain Mapp. 30, 1857–1865. doi:10.1002/hbm.20745
Sporns, O., Chialvo, D.R., Kaiser, M., Hilgetag, C.C., 2004. Organization, development and function of complex brain networks. Trends Cogn. Sci. 8, 418–425.
Stam, C.J., 2014. Modern network science of neurological disorders. Nat. Rev. Neurosci. 15, 683–95. doi:10.1038/nrn3801
Stam, C.J., Nolte, G., Daffertshofer, A., 2007. Phase lag index: assessment of functional connectivity from multi channel EEG and MEG with diminished bias from common sources. Hum. Brain Mapp. 28, 1178–93. doi:10.1002/hbm.20346
Stam, C.J., Tewarie, P., Van Dellen, E., van Straaten, E.C.W., Hillebrand, A., Van Mieghem, P., 2014. The trees and the forest: Characterization of complex brain networks with minimum spanning trees. Int. J. Psychophysiol. 92, 129–138. doi:10.1016/j.ijpsycho.2014.04.001
Stam, C.J., van Straaten, E.C.W., 2012. The organization of physiological brain networks. Clin. Neurophysiol. 123, 1067–87. doi:10.1016/j.clinph.2012.01.011
Steen, F. Van de, Faes, L., Karahan, E., Songsiri, J., 2016. Critical comments on EEG sensor space dynamical connectivity analysis. Brain Topogr. Epub ahead of print.
Tadel, F., Baillet, S., Mosher, J.C., Pantazis, D., Leahy, R.M., 2011. Brainstorm: a user-friendly application for MEG/EEG analysis. Comput. Intell. Neurosci. 2011, 879716. doi:10.1155/2011/879716
Tewarie, P., Hillebrand, A., Schoonheim, M., Van Dijk, B., Geurts, J., Barkhof, F., Polman, C., Stam, C., 2014. Functional brain network analysis using minimum spanning trees in Multiple Sclerosis: an MEG source-space study. Neuroimage 88, 308--318.
Tewarie, Dellen, V., Hillebrand, Stam, 2015. The minimum spanning tree: An unbiased method for brain network analysis. Neuroimage 104, 177–188. doi:10.1016/j.neuroimage.2014.10.015
van Dellen, E., Douw, L., Hillebrand, A., de Witt Hamer, P.C., Baayen, J.C., Heimans, J.J., Reijneveld, J.C., Stam, C.J., 2014. Epilepsy surgery outcome and functional network alterations in longitudinal MEG: a minimum spanning tree analysis. Neuroimage 86, 354–63. doi:10.1016/j.neuroimage.2013.10.010
van Diessen, E., Otte, W.M., Stam, C.J., Braun, K.P.J., Jansen, F.E., 2016. Electroencephalography based functional networks in newly diagnosed childhood epilepsies. Clin. Neurophysiol. 127, 2325–2332. doi:10.1016/j.clinph.2016.03.015
Van Mieghem, P., Magdalena, S.M., 2005. Phase transition in the link weight structure of networks. Phys. Rev. E 72, 56138. doi:10.1103/PhysRevE.72.056138
Van Mieghem, P., van Langen, S., 2005. Influence of the link weight structure on the shortest path. Phys. Rev. E 71, 56113. doi:10.1103/PhysRevE.71.056113
van Wijk, B.C.M., Stam, C.J., Daffertshofer, A., 2010. Comparing brain networks of different size and connectivity density using graph theory. PLoS One 5, e13701. doi:10.1371/journal.pone.0013701
Vourkas, M., Karakonstantaki, E., Simos, P.G., Tsirka, V., Antonakakis, M., Vamvoukas, M., Stam, C., Dimitriadis, S., Micheloyannis, S., 2014. Simple and difficult mathematics in children: A minimum spanning tree EEG network analysis. Neurosci. Lett. 576, 28–33. doi:10.1016/j.neulet.2014.05.048

Wang, H., Hernandez, J.M., Van Mieghem, P., 2008. Betweenness centrality in a weighted network. Phys. Rev. E 77, 46105. doi:10.1103/PhysRevE.77.046105

Wilcox, R.R., 2016. Comparing dependent robust correlations. Br. J. Math. Stat. Psychol. 69, 215–224. doi:10.1111/bmsp.12069

Yu, M., Gouw, A.A., Hillebrand, A., Tijms, B.M., Stam, C.J., van Straaten, E.C.W., Pijnenburg, Y.A.L., 2016. Different functional connectivity and network topology in behavioral variant of frontotemporal dementia and Alzheimer's disease: an EEG study. Neurobiol. Aging 42, 150–162. doi:10.1016/j.neurobiolaging.2016.03.018